UNIVERSIDAD REGIONAL AMAZÓNICA IKIAM

Facultad de Ciencias de la Tierra y Agua

Carrera de Hidrología

Comparación entre los métodos EPIK y DRASTIC para evaluar la vulnerabilidad de la Formación Kárstica Napo, cuenca occidental del río Amazonas (Ecuador)

Elizabeth Estefanía Naranjo Garófalo

Tena, enero 2022.

Napo, Ecuador.

Declaración de derecho de autor, autenticidad y responsabilidad

Tena, 14 de septiembre de 2021

Yo, Elizabeth Estefanía Naranjo Garófalo con documento de identidad N°1722647227, declaro que los resultados obtenidos en la investigación que presento en este documento final, previo a la obtención del título Ingeniero en Ciencias del Agua según el Art. 22 del Reglamento de Titulación son absolutamente inéditos, originales, auténticos y personales.

En virtud de lo cual, el contenido, criterios, opiniones, resultados, análisis, interpretaciones, conclusiones, recomendaciones y todos los demás aspectos vertidos en la presente investigación son de mi autoría y de mi absoluta responsabilidad.

Por la favorable atención a la presente, suscribo de usted,

Atentamente,

Firma:

Elizabeth Naranjo

_____
Elizabeth Estefanía Naranjo Garófalo

Certificado de dirección de trabajo de integración curricular

Certifico que el trabajo de integración curricular titulado: "Comparación entre los métodos EPIK y DRASTIC para evaluar la vulnerabilidad de la Formación Kárstica Napo, cuenca occidental del río Amazonas (Ecuador)", en la modalidad de: proyecto de investigación en formato artículo original, fue realizado por: Elizabeth Estefanía Naranjo Garófalo, bajo mi dirección.

El mismo ha sido revisado en su totalidad y analizado por la herramienta de verificación de similitud de contenido; por lo tanto, cumple con los requisitos teóricos, científicos, técnicos, metodológicos y legales establecidos por la Universidad Regional Amazónica Ikiam, para su entrega y defensa.

Tena, 14 de septiembre de 2021

Firma:

Firmado electrónicamente por:
BRUNO PIRILO

……………………………
Bruno Pirilo Conicelli
C.I: 1759149774
Tutor

INVESTIGACIÓN | Parroquia Muyuna, kilómetro 7 vía a Alto Tena
INNOVACIÓN | Tena · Napo · Ecuador
EDUCACIÓN | **Telf.:** (06) 370 0040 · (06) 299 9160

www.ikiam.edu.ec
@u_ikiam   IkiamOficial   u_ikiam   Universidad Ikiam

ii

AGRADECIMIENTOS

''Nuestra recompensa se encuentra en el esfuerzo y no en el resultado. Un esfuerzo total, es una victoria completa''   - Mahatma Gandhi

Al concluir esta etapa de mi vida quiero extender un profundo agradecimiento a quienes formaron parte de este sueño.

En primer lugar, considero que merezco un agradecimiento propio. Como una especie de palmadita en la espalda por un logro conseguido que pesar de tener mucho apoyo, la victoria y la satisfacción por ello es de uno mismo. Existieron ocasiones en las que quieres rendirte, pero encuentras ese coraje para continuar. La universidad, para mí fue como escalar una montaña, se te presentan ocasiones en las que resbalas y caes, pero encuentras algo de donde sostenerte y continúas subiendo hasta que llegas a la cima y pues disfrutar de la vista con orgullo.

Es necesario agradecer el primer apoyo que recibes siempre, el que viene de tus padres, en mi caso, mi padre. No hay palabras para expresar el agradecimiento y gratitud hacia mi padre por todo su apoyo incondicional en esta aventura llamada universidad. Gracias por creer y confiar en mí, todo lo que he logrado ha sido gracias a él. Se lo duro que fue para el dejarme ir a otra ciudad sola, siempre hubo momentos en los que quería que volviera, pero al final se resignó.

Un profundo agradecimiento a todos los profesores quienes se esforzaron por transmitirnos su conocimiento e interés por la ciencia y la investigación que iba más allá de lo abordado en clase. Especialmente a mi tutor, el PhD. Bruno Conicelli por la confianza, el apoyo y paciencia durante la elaboración de este proyecto.

Quiero agradecer a mis amiguitos por todo su apoyo y amistad durante toda la carrera, en especial a Carlos, Jusseth y Brian. Siempre recordare las reuniones de proyectos en las que, aunque Juss no compartía clases con nosotros siempre estaba ahí para apoyarnos. Las risas, aventuras y momentos compartidos siempre los llevare conmigo.

Agradezco a Sebastián por su amistad desde el primer día, a Zuri, Estefy por la motivación, la amistad y por siempre estar ahí para mí.

Gracias infinitas, Eli

DEDICATORIA

Dedico este trabajo a:

Mi padre, por el apoyo incondicional.

Mi gato porque sin saberlo me daba el apoyo, la motivación y la compañía que necesitaba.

Mis amigos Carlos, Brian, Jusseth por la amistad y por convertirse en mi segunda familia.

La música y BTS que me acompaño en la redacción de este documento.

ÍNDICE GENERAL

ÍNDICE DE FIGURAS

ÍNDICE DE TABLAS

RESUMEN:

Los ambientes kársticos son susceptibles a la contaminación, afectados directamente por presiones antropogénicas como la minería, la extracción de petróleo y la agricultura extensiva. Los mapas de vulnerabilidad permiten generar zonas de protección considerando que el proceso de remediación podría ser costoso y largo. Por lo tanto, este estudio tiene como objetivo evaluar la vulnerabilidad de la Formación Kárstica Napo utilizando índices de vulnerabilidad. Para esto se consideraron dos índices: (i) EPIK, (ii) DRASTIC, y un DRASTIC modificado, DRASTIC-LUC.

Los resultados muestran que DRASTIC (45.76%) y EPIK (35.38%) consideran a la zona de estudio como altamente vulnerable mientras que DRASTIC-LUC la muestra como moderadamente vulnerable (57.47%). La diferencia entre los métodos radica en los parámetros que modelo emplea y como calcula cada uno la vulnerabilidad. Además, es necesario considerar que la asignación de cada parámetro está sujeta a la subjetividad porque depende del conocimiento del autor y de los datos disponibles. El análisis de sensibilidad para evaluar la subjetividad en conjunto con el análisis espacial muestra que DRASTIC-LUC es el mejor método que se adapta a la zona de estudio porque el error en los datos empleados es menor e incluye un parámetro importante como la cobertura y uso de suelo. Los resultados obtenidos pueden servir de base para futuros estudios centrados en la validación de la metodología empleada. De igual forma, pueden incluirse en estudios técnicos para la toma de decisiones sobre actuaciones que puedan afectar directamente a la calidad de las aguas superficiales y subterráneas.

Palabras clave: Vulnerabilidad del Agua Subterránea; EPIK; DRASTIC; Análisis de Sensibilidad; Amazonía

ABSTRACT:

Karst environments are susceptible to contamination and directly affected by anthropogenic pressures such as mining, oil extraction, and extensive agriculture. Vulnerability maps allow the generation of protection zones, considering that the remediation process could be costly and time-consuming. Therefore, this study aims to evaluate the vulnerability of the Napo karst formation using vulnerability indices. For this, two indices were considered: (i) EPIK, (ii) DRASTIC, and a modified DRASTIC, DRASTIC-LUC.

The results show that DRASTIC (45.76%) and EPIK (35.38%) consider the study area highly vulnerable, while DRASTIC-LUC shows it as moderately vulnerable (57.47%). The difference between the methods lies in the parameters that the model uses and how each one calculates vulnerability. In addition, it is necessary to consider that the assignment of each parameter is subject to subjectivity because it depends on the author's knowledge and available data. The sensitivity analysis to evaluate subjectivity in conjunction with the spatial analysis shows that DRASTIC-LUC is the best method to adapt to the study area because the error in the data used is lower and it includes important parameters such as land cover and land use. The results obtained can serve as a basis for future studies focused on the validation of the methodology used. Similarly, they can be included in technical studies for decision-making on actions that may directly affect the quality of surface and groundwater.

Keywords: Groundwater vulnerability; EPIK; DRASTIC; Sensitivity analysis; Amazon

GRAPHICAL ABSTRACT:
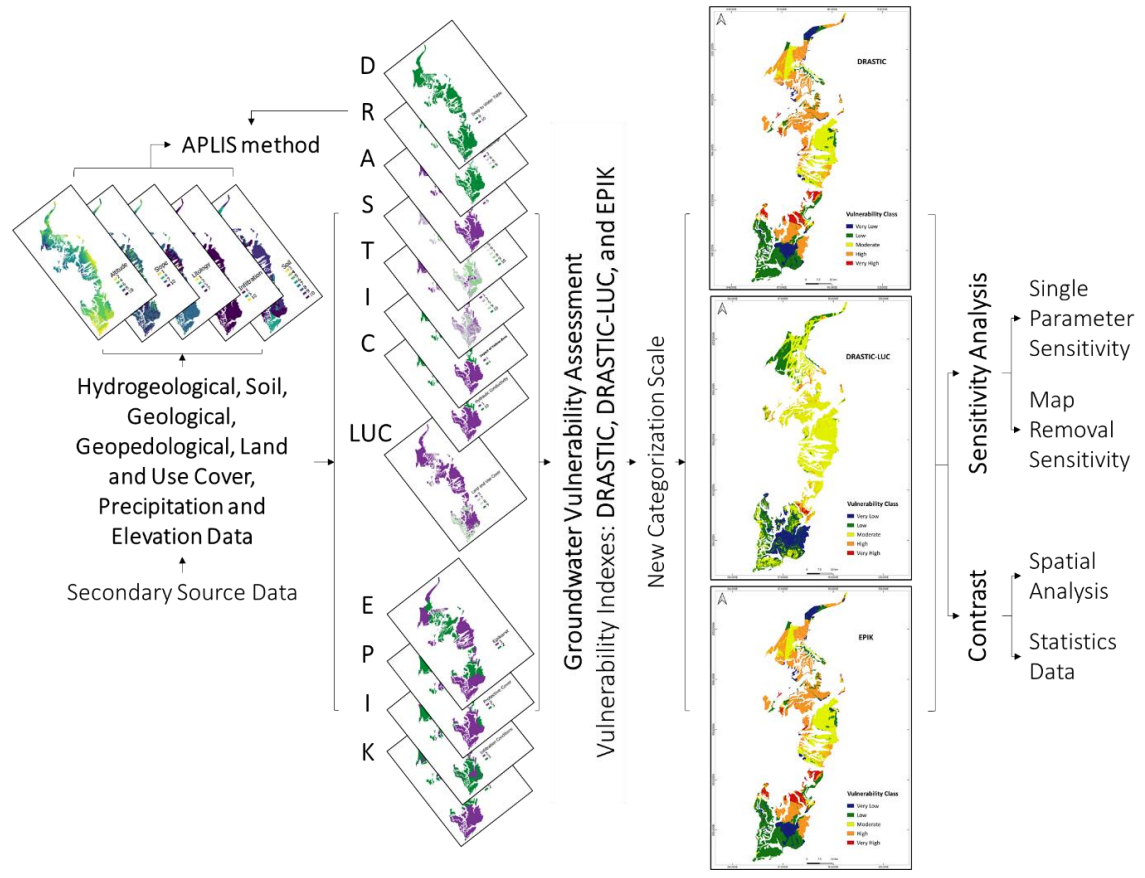
Comparación entre los métodos EPIK y DRASTIC para evaluar la vulnerabilidad de la Formación Kárstica Napo, cuenca occidental del río Amazonas (Ecuador)

1. Introduction

Groundwater pollution, which directly affects water supply, has become a growing concern in recent years (Hadžić et al., 2015). For example, aquifers, caves, caverns, and surface karst features can be contaminated by rural and urban development (Onac and van Beynen, 2020). Karst aquifers cover around 15.2% of the land surface of the Earth (Goldscheider et al., 2020) and are available in different climatic conditions, mainly in arid areas (34.2%). However, a small percentage of them occur in tropical regions (13.1%). In South America, 58.7% of the total carbonate rock areas have karst aquifers (Goldscheider et al., 2020).

The importance of the karst aquifers is that they provide water for about 25% of the global population (Goldscheider, 2005; Kalhor et al., 2019). In addition, the water from this type of aquifer is characterized by its high quality and often does not require costly treatment (Stevanović, 2018). However, the characteristics that distinguish karst aquifers (Duarte et al., 2013; Jiménez-Madrid et al., 2019) and the lack of hydrogeological studies lead everyone wrongly to consider karst water sources pollution free (Constantin et al., 2018). Another factor to consider is that the development of above-ground activities can threaten groundwater quality, making karst aquifers extremely vulnerable to pollution compared to other hydrogeological environments (Foster et al., 2002; Ravbar and Goldscheider, 2009).

In Ecuador, groundwater is primarily used for domestic supply and, secondarily, for industrial purposes and irrigation. Groundwater is important in sixteen cities (among the main ones are Tulcán, Ibarra, Ambato, Riobamba, Guaranda, Latacunga, Quito, Arenillas, Machala, Huaquillas, Milagro), particularly for domestic use (Burbano et al., 2015; Rebouças, 1999). Ecuador's most crucial groundwater source is the Amazon region (Buckalew et al., 1998). Amazon region is characterized by high precipitation levels (2500–3000 mm/year) (INAMHI, 2013; Villacís et al., 2008). This allows karstification process to take place, giving rise to different structures characteristic of karst environments (Andreo et al., 2010; Stevanović, 2015).

According to Constantin et al. (2018), carbonate rocks in Ecuador represent between 5 and 10% of the land surface. The Amazon Karst System (AKS) is formed by many limestone or karst caves in the Amazon region that remain understudied, probably because of the dense vegetation that makes them inaccessible (Chamba, 2020). The AKS is exposed to environmental impacts caused by mining,

extensive agriculture, non-native fish farming, lack of basic infrastructure, and oil extraction (Lessmann et al., 2016). Moreover, ecological deterioration in the Amazon has increased as pollution sources have multiplied as the population has grown and economic activity has become more diverse (Pimm et al., 2014 as cited by Capparelli et al., 2019).

A previous study by Capparelli et al. (2019) suggested that anthropogenic activities introduced metals into aquatic systems. In a new study, their results demonstrate that medium-scale to industrial-scale gold mining has impacted the quality of aquatic ecosystems in the Napo River and that the water is not recommended for human consumption (Capparelli et al., 2021). In addition, there is the presence of new emerging pollutants. For example, Lucas-Solis et al. (2021) attribute the presence of microplastics in the upper Amazon River basin to the deficient wastewater treatment plants, the mismanagement of solid waste in landfills, and the constant load of domestic waste outfall into the Misahuallí River and its tributaries. On the other hand, in the lower Napo River basin, the pollutants derived from oil exploration and extraction in the surrounding areas of Aguarico River may impact soil, groundwater, and surface water (Merchán and Chiogna, 2017).

Because remediation processes could be costly and take a long time, the most reliable protection of groundwater is to prevent pollution (Hadžić et al., 2015). Thus, the term ''vulnerability assessment'' was introduced. The central concept of Groundwater Vulnerability Assessment (GVA) is to prioritize areas based on their pollution vulnerability (Ramaraju and Krishna Veni, 2017). To evaluate vulnerability, it is necessary to consider that there are two types of vulnerability: specific and intrinsic. The specific vulnerability is considered to be the likelihood that the aquifer could be polluted by a specific or group of pollutants that are introduced into the ground surface through human activities (Barzegar et al., 2020; Panagopoulos et al., 2006). On the other hand, an intrinsic vulnerability refers to the predisposition of an aquifer to pollution quantified only in terms of its hydrogeological (Jarrín et al., 2017). This study considers only intrinsic vulnerability. This vulnerability analysis does not consider the source of the pollutants and their specific nature, but instead focuses on the natural environment's inherent geological, hydrological, and hydrogeological properties (Abiy et al., 2016).

The GVA using spatial evaluation is crucial to protect and prevent groundwater pollution (Hadžić et al., 2015; Kumar and Krishna, 2020). For example, using thematic maps of groundwater vulnerability provides a way to understand the vulnerability derived from anthropogenic activities (Talozi and Hijazi, 2013). These maps are considered essential instruments for groundwater management because they provide decisive information to facilitate proper planning and

2

protection (Majandang and Sarapirome, 2013). It means that GVA can consolidate highly complex technical information about hydrogeologic and pollutants into a language that planners, decision-makers, and the general public can use (Baloch and Sahar, 2014). From the point of view of groundwater protection, it is essential to define and map the areas with a potential risk of pollution (Hadžić et al., 2015). For all of the above reasons, the protection of groundwater resources is imperative, especially in karst areas (Pacheco et al., 2018). In this regard, this study aims to assess the vulnerability present in the Napo Karstic Formation using vulnerability indices and GIS techniques. This action allows approximate groundwater vulnerability mapping without significant economic investment (Sahoo et al., 2016).

2. Study site

The Napo Karstic Formation (NKF) has an estimated area of 2096 km^2 and is part of the karstic formations of South America, many of them inside the Amazon River basin, Fig. 1a. Within the Ecuadorian territory, it is found mainly in the province of Napo and small parts of Sucumbíos and Orellana, Fig. 1b.
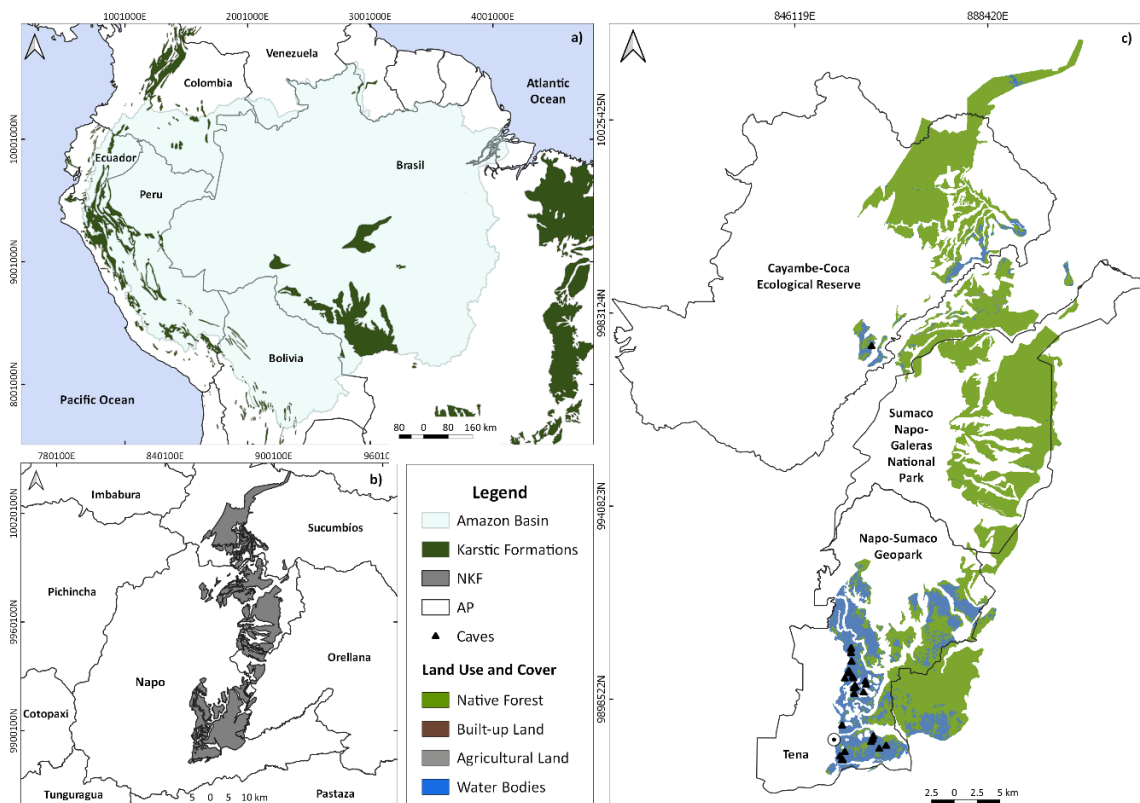

Fig. 1. Study area. **a)** Karstic Formations in South America and the Amazon Basin, **b)** Napo Karstic Formation (NKF) at Napo province, Ecuador, **c)** Protected areas, Land Use and Cover, Karstic Caves in the NKF.

As shown in Fig. 1c., the NKF is located within protected areas: 28% are inside Sumaco Napo-Galeras National Park, 23% in the Cayambe-Coca Ecological Reserve, and 26% in the Napo-Sumaco Geopark. In the study area, the altitude ranges from 370 to 3039 masl. According to Espol Tech EP (2014), NKF lithology comprises black shales, limestone, and calcareous sandstones. The aquifers in NKF could be local or discontinuous (Constantin et al., 2018), shallow, with high flow velocity, and connected directly with the surface (Espol Tech EP, 2014).

3. Materials and methods
3.1. Data collection and processing

Geographical data, such as thematic maps, used for this study came from secondary sources of data. All the data was collected from the different platforms of the governmental entities in charge of producing this type of data. The information was incorporated and processed with QGIS 3.12.3 La Coruña.

In this way, some missing data was filled in with similar information. For example, geopedological shapefiles from the years 2016 and 2019 were compared for the study area. Under the assumption that both shapefiles contained the same variables, the information available for both years was merged. In addition, the information used to determine some parameters was not available for the protected areas in the study area. This required a comparison with similar information developed in previous years. The other changes and adaptations made to some of the parameters are detailed below.

Table 1
Data collected for obtaining the parameters of each methodology.

Data	Source
Land Use and Cover, Protected Areas – Shapefile (1:100.000)	Ministry of the Environment and Water (MAAE), Unique Environmental Information System (SUIA) (http://suia.ambiente.gob.ec)
Hydrogeologic, Soil, Geological, and Geopedological Data – Shapefile (1:100.000)	Ministry of Agriculture, Livestock, Aquaculture and Fisheries (MAGAP) (http://geoportal.agricultura.gob.ec), National Information System (SNI) (https://sni.gob.ec/coberturas)
STRM Worldwide Elevation Data - *DEM (30 m), South American Geology - Shapefile	United States Geological Survey (USGS), USGS website (www.earthexplorer.com) (https://catalog.data.gov)
Monthly Precipitation Average (1970-2000) - Raster 30 sec (~ 1 km^2)	WorldClim 2.1 (Fick and Hijmans, 2017) (https://worldclim.org)

*Digital Elevation Model

The methodology was designed to: (1) collect data from relevant sources and prepare each parameter for the vulnerability index computation; (2) generate vulnerability maps using DRASTIC,

DRASTIC-LU, and EPIK; and (3) perform sensitivity analysis as an efficiency indicator. Fig. 2., shows the flowchart developed for the methodology.
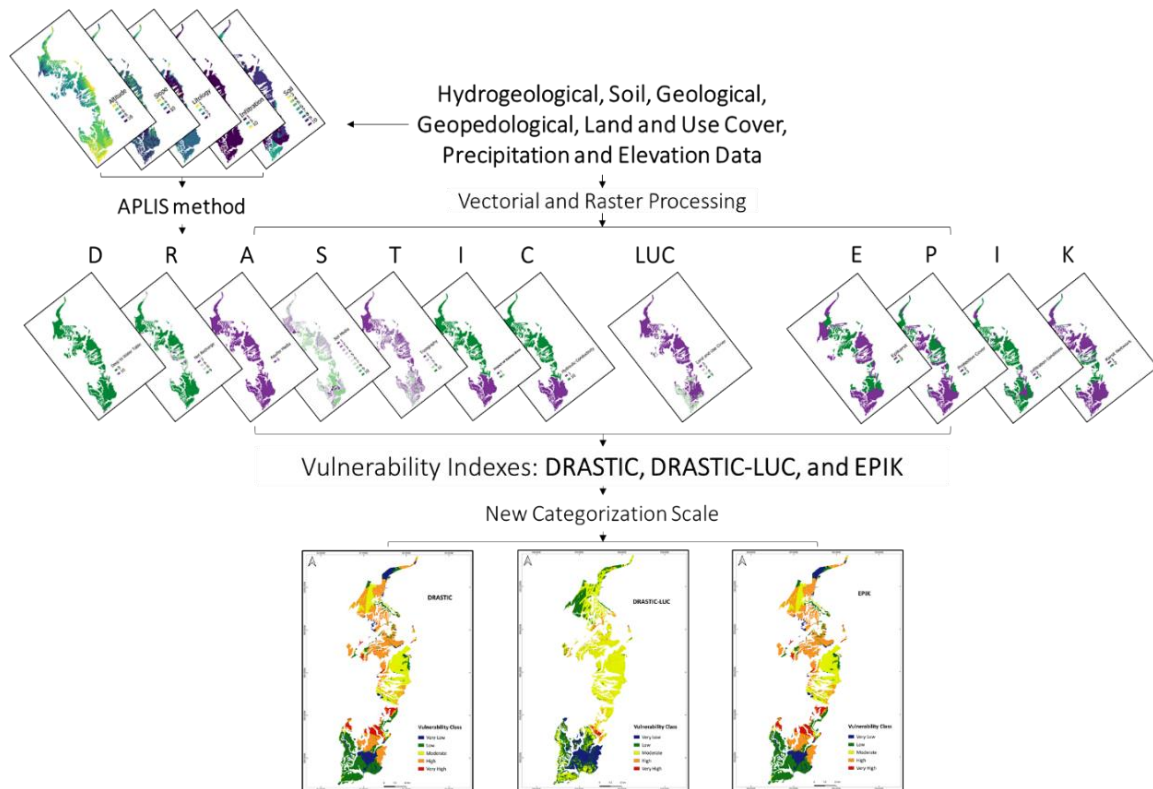
Fig. 2. Flowchart of the overall methodology.

3.2. Vulnerability methods

GVA is not a characteristic that can be directly measured in the field (Gogu and Dassargues, 2000a). This led some authors to develop different methods to evaluate vulnerability according to geographical or hydrogeological conditions. The final vulnerability map is created through overlaying the individual characteristics using QGIS (Shirazi et al., 2013). For this study, two methods were considered: one specific to karstic environments (EPIK) and another applied to any hydrogeological setting (DRASTIC). Also, it was considered a DRASTIC modified, DRASTIC-LUC, which included Land Use and Cover.

3.2.1. DRASTIC Method

The DRASTIC method was developed by Aller et al. (1987). It is calculated roughly analogous to the likelihood that pollutants released in a region reach the groundwater. So that implies that a high value is directly related to the probability of pollution (Shirazi et al., 2013; Talozi and Hijazi, 2013). DRASTIC is the most commonly used method for mapping groundwater vulnerability. Vulnerability maps using DRASTIC have become popular in recent years and have been applied to different

environments and show promising results in Algeria (Boufekane and Saighi, 2018), Tunisia (Ayed et al., 2017), Bangladesh (Hasan et al., 2019), India (Khan and Jhariya, 2019), Pakistan (Maqsoom et al., 2020), Nigeria (Oke, 2020), Iran (Oroji and Karimi, 2018), and England (Moustafa, 2019). For example, in a local context, Coello and Galárraga (2002) used the DRASTIC index in the North Quito Aquifer to determine its susceptibility to pollution.

The acronyms of DRASTIC refer to seven hydrogeological parameters such as (D) depth to groundwater, (N) net recharge, (A) aquifer media, (S) soil media, (T) topography, (I) impact on the vadose zone, and (C) hydraulic conductivity (Pathak et al., 2009). Equation (1) describes how to calculate DRASTIC using the seven parameters:

$$\textbf{Drastic index } = \textbf{D}_\textbf{w} \cdot \textbf{D}_\textbf{r} + \textbf{R}_\textbf{w} \cdot \textbf{R}_\textbf{r} + \textbf{A}_\textbf{w} \cdot \textbf{A}_\textbf{r} + \textbf{S}_\textbf{w} \cdot \textbf{S}_\textbf{r} + \textbf{T}_\textbf{w} \cdot \textbf{T}_\textbf{r} + \textbf{I}_\textbf{w} \cdot \textbf{I}_\textbf{r} + \textbf{C}_\textbf{w} \cdot \textbf{C}_\textbf{r} \qquad (1)$$

The subscripts r and w are the rating and weight for each parameter, respectively, summarized in Table 2. Furthermore, DRASTIC assumes certain conditions, such as (1) pollutants are introduced through the soil, (2) precipitation carries pollutants into the groundwater, (3) pollutants move with the water, and (4) the assessment area is equal to or greater than 0.4 km^2 (Shirazi et al., 2013; Talozi and Hijazi, 2013).

Table 2
Rating, ranges, and weight of each DRASTIC and DRASTIC-LU parameter.

Thematic Layer	Symbol	Range	Rating	Symbol	Weight
Depth to Water Table (m)	D_r	0 - 1.5	10	D_w	5
		1.5 - 4.6	9		
Net Recharge (mm)	R_r	50 – 103	3	R_w	4
		103 – 178	6		
		178 – 254	8		
		> 254	9		
Aquifer Media	A_r	Sandstone, Limestone and Shale sequence	6	A_w	3
Soil media	S_r	Thin or Absent	10	S_w	2
		Loamy sand	9		
		Loam	8		
		Sandy loamy	7		
		Silty loam	6		
		Clay loam	5		
		Sandy clay loam, Silty clay loam	4		
		Silty	3		
		Sandy clay, Silty clay	2		
		Clay, Heavy clay	1		
Topography (%)	T_r	0 – 2	10	T_w	1

		2.0 - 6.0	9		
		6.0 - 12.0	5		
		12.0 - 18.0	3		
		> 18.0	1		
Impact of Vadose Zone	I_r	Shale	3	I_w	5
		Limestone	6		
Hydraulic Conductivity (mm/day)	C_r	0.04 - 4.8	1	C_w	3
		> 81.49	10		

Depth to water table could be defined as the distance from the ground surface to the water table (Al-Zabet, 2002). There is an inverse relationship between the depth of the water table and the pollution possibility. Therefore, a deeper water table level implies fewer pollution (Kumar and Krishna, 2020; Zghibi et al., 2016). Moreover, it is considered relevant to the depth of the material through which any pollutant travels before reaching the aquifer (Al-Zabet, 2002). This parameter was obtained from the geopedological shapefile that contains a variable denominated depth to the water table (MAGAP, 2015).

Net recharge is the amount of recharge that is positively correlated with the vulnerability rating (Jang et al., 2017; Saidi et al., 2010; Zghibi et al., 2016). Net recharge includes the average annual amount of infiltration without considering the distribution, intensity, or duration of recharge events (Al-Zabet, 2002). Due to the lack of information for this parameter, the APLIS method was used. The method developed by Andreo et al. (2004) evaluates the mean annual recharge in carbonate aquifers (Zagana et al., 2011). It is expressed as the percentage of precipitation that infiltrates the soil. The APLIS method was applied to a karst aquifer terrain in Cuba (Farfán et al., 2010), the Amazon region of Perú (Espinoza et al., 2015) and produced acceptable results. The APLIS method uses the following variables such as altitude (A), slope (P), lithology (L), infiltration (I), and soil (S). After the necessary process, the final map is calculated with equation (2):

$$\mathbf{R = (A + P + 3 \cdot L + 2 \cdot I + S)/0.9} \tag{2}$$

The APLIS method was developed for arid areas, so modifications and adaptations were necessary for this study. These changes were applied to lithology, infiltration, and soil according to Napo Formation conditions. For example, in preferential infiltration, it was necessary to consider geologic faults and caverns, mapped by Sánchez Cortez (2017), as preferential infiltration areas and give them a value of 10. Moreover, on the other hand, the rest of the regions acquire valor of 5. Similar considerations were applied in Zagana et al. (2011) and Entezari et al. (2020). Table 3 contains the rating and range for each parameter and the adaptions mentioned above.

Table 3
The range and rating of each parameter adapted from Andreo et al. (2008).

Thematic Layer	Symbol	Range	Rating
Altitude (m)	A	300 - 600	2
		900 - 1200	4
		1500 - 1800	6
		2100 - 2400	8
		≥ 2700	10
Slope (%)	P	≤ 3	10
		16 -21	7
		31 - 46	4
		>100	1
Litology	L	Limestones	7
		Shales	6
		Sands, gravels	5
		Granite, gneiss, methamorphic and intrusive rocks	4
		Fine materials, conglomerates	3
		Schists, slates, slimes, clays, clay slates	2
		Basalts, ashes, andesites	1
Infiltration	I	Geological faults	10
		Caverns	10
		Rest	5
Soil	S	Andosols	10
		Umbrisols	9
		Leptosols	8
		Regosols	7
		Cambisols	6
		Stagnosols	5
		Gleysols	4
		Fluvisols	3

In addition, to obtain the amount of recharge (in mm), it is necessary to consider precipitation data. However, because the available data (1980-2010) only covered accumulated precipitation, and meteorological station data were incomplete, it was impossible to use information from the INAMHI. Consequently, it employed the average monthly rainfall for 1970-2000 from WorldClim (Table 1). Current data (2000-2010) were available at a different scale ~340 km^2. Therefore, to calculate the amount of rainfall, equation (3) was used. So, the recharge obtained is considered a factor (recharge%/100%) multiplied by the precipitation raster.

$$\textbf{Net Recharge} = (\% \textbf{ Recharge}/\textbf{100}\%) \cdot \textbf{Precipitation isohyet} \tag{3}$$

Aquifer media is the rock material that serves as an aquifer inside the saturated zone (Saida et al., 2017), where the material properties control the pollutant attenuation processes (Awawdeh et al.,

2015). This parameter is related to the permeability that is controlled by the geological characterization (Al-Zabet, 2002; Zghibi et al., 2016). Thus, a high permeability allows more water and, therefore, more pollutants to enter the aquifer (Bhuvaneswaran and Ganesh, 2019). In Table 2, it is possible to establish the rating and range for this parameter based on the hydrogeological shapefile of the study area.

Soil media is the first zone that water or any pollutant passes through when it percolates into the ground. For that reason, soil properties affect water transportation from the surface to the aquifer (Jang et al., 2017; Ouedraogo et al., 2016). Specifically, soil texture is the property that impacts the amount of recharge into the ground (Khosravi et al., 2018; Zghibi et al., 2016). This parameter was constructed using a geopedological and soil texture shapefile for the study area (MAGAP, 2015). So, the soil order data was under the USDA (United States Department of Agriculture) taxonomy while the methodology used the WRB 2015 (World Reference Base) taxonomy. This led to a change from one taxonomy to another based on bibliographic information and considering evolution, texture, and thickness characteristics. And, to avoid using incorrect data, all of them were reviewed one by one to be consistent with the characteristics of the study area.

Topography determines the runoff and infiltration capacity of the water into the soil (Ouedraogo et al., 2016). Furthermore, it influences whether or not a pollutant can infiltrate the ground and allows the user to obtain geographic information about its concentration (Davis et al., 2002; Shirazi et al., 2013). The most important topographic parameter required is slope, which was estimated from a DEM using GDAL tools. The range and rating for this parameter are the same as those used in the original methodology for DRASTIC.

Impact of the vadose zone. The vadose zone could be defined as the space between the water table and the ground surface (Jang et al., 2017; Shirazi et al., 2013). It is an essential parameter in the vulnerability assessment because it influences the residence time of the pollutants in the unsaturated zone (Ouedraogo et al., 2016; Shirazi et al., 2013). To estimate this parameter, the hydrogeological and geopedological shapefiles for the study area that contain a variable named lithology were compared and used. Here, considering the information above, it was only necessary to place the value obtained from the original DRASTIC methodology.

Hydraulic conductivity is the capacity of an aquifer to allow fluids (water, any pollutant) to pass through it and regulate their movement in the saturated zone (Al-Zabet, 2002; Shirazi et al., 2013). In addition, hydraulic conductivity is positively correlated with the vulnerability rating (Hasan et al., 2019; Jang et al., 2017; Khosravi et al., 2018; Zghibi et al., 2016). For this parameter, it is necessary

to obtain aquifer data (transmissivity, grain size information, and thickness) to obtain the permeability, which is the same as the hydraulic conductivity, and that could be estimated from well data and pump tests. Nonetheless, when there is no information available, it is possible to use theoretical tables. Hydraulic conductivity values were assigned considering values by Freeze and Cherry (1979) for each lithology (derived from the geopedological and hydrogeological shapefile). The range and rating assigned are depicted in Table 2.

3.2.1.1.   DRASTIC-LUC Method

DRASTIC-LU is a modified DRASTIC that includes Land Use and Cover. It is used to assess groundwater vulnerability while taking land use and cover into account (Umar et al., 2009), which means how human activities have impacted karstic and non-karstic areas. This method has primarily been used in India, with positive results (Alam et al., 2014; Kumar and Krishna, 2020; Sahoo et al., 2016; Wei et al., 2021).

Land Use and Cover (LUC) could be defined as the cover over the soil and the activities there. The water that has percolated through the soil, reaching an unsaturated zone, can also transport anthropogenic pollutants (Lerner and Harris, 2009). Groundwater quality can be influenced by human actions. For example, inefficient wastewater treatment, agricultural activities, mining, and industrial tailings change the physical and chemical composition of water and increase its vulnerability (Ramaraju and Krishna Veni, 2017). On the other hand, changes in land cover affect the available resources by changing recharge rates (Lerner and Harris, 2009). A shapefile with information about land use and cover from 2018 was considered for the study area. Equation (4) shows how DRASTIC-LUC is calculated.

$$\mathbf{DRASTIC - LUC = Drastic\ Index + LUC_r \cdot LUC_w} \tag{4}$$

Where the subscripts r and w are the rating and weight for each parameter, respectively. DRASTIC-LUC assigned a low value to natural areas (forests) and high values to agricultural, urban, and water bodies. The values assigned are shown in Table 4 and their distribution in Fig. 1c.

Table 4
Rating, ranges, and weight for LUC parameter inside of DRASTIC-LUC index.

Parameter	Symbol	Range	Area %	Rating	Symbol	Weight
Land Use and Cover	LU_r	Native Forest, Herbaceous Vegetation	78.91	3	LU_w	5
		Built-Up Land	0.18	5		
		Populated Area, Agricultural Land	20.62	7		
		Water Bodies	0.28	9		

3.2.2. EPIK Method

Intrinsic vulnerability assessment in karst areas requires a method that considers geomorphological, hydrological, and hydrogeological characteristics (de Castro and Menegasse, 2017; Gogu and Dassargues, 2000b). The EPIK method was chosen because it is one of the most widely used methods for vulnerability assessment that is specific to karst environments (Hammouri and El-Naqa, 2008). EPIK was developed by Doerfliger and Zwahlen (1998). It is an acronym for epikarst (E), protective cover (P), infiltration conditions (I), and karst network development (K).

A multi-attribute weighting-rating method (Doerfliger et al., 1999) analyzes four parameters individually and combines them using a raster calculator (Doummar et al., 2012). Also, this method has been applied in different environments such as Brazil (Lenhare and Sallun Filho, 2019; Pereira et al., 2019), Algeria (Nekkoub et al., 2020), Morocco (Alili et al., 2018), Greece (Vogelbacher et al., 2019). The final product is the protection factor (F). Here, a low F value represents high vulnerability, while a high F value shows low vulnerability (Marín and Andreo, 2015). The index is calculated with the equation:

$$F_i = (\propto \cdot E_i) + (\beta \cdot P_i) + (\gamma \cdot I_i) + (\delta \cdot K_i) \tag{5}$$

Where, F_i is the protection factor for each subarea i, α, β, γ, α, δ are the weighting factor for each parameter E, P, I, and K. Table 5 contains the value assigned for the weighting as mentioned earlier and the rating for each parameter. The ratings for each class of a given attribute are multiplied by the weight related to the point, and then the products are added up to arrive at a final score (Doerfliger et al., 1999).

Table 5
Values for each EPIK parameter were obtained from Doerfliger and Zwahlen (1998).

Parameter	Symbol	Range	Rating	Symbol	Weight
Epikarst	E_1	Sinkholes or dolines, karren, polje, caves, springs	1	$\propto$	3
	E_2	Intermediate zones along doline alignments	2		
Protective Cover	P_2	20 - 100 cm of soil with low hydraulic conductivity	2	β	2
	P_3	> 1 m of soil with low hydraulic conductivity	3		
Infiltration Conditions	I_2	The slope is more than 10% for cultivated areas and less than 25% for meadows and pastures	1	γ	1
	I_3	The slope is less than 10% for cultivated areas and less than 25% for meadows and pastures	2		
Karst Network	K_1	Well-developed karstic network with little fill and well-interconnected conduits	1	δ	3
	K_2	Poorly karstic network with poorly interconnected or infilled drains or conduits	2		

Epikarst is the karstified zone under the soil cover. In some areas, this is open to the surface (Bakalowicz, 2019; Doummar et al., 2012; Stevanović, 2015). Furthermore, it controls the infiltration into the aquifer and stores water (Goldscheider, 2005). The geomorphological information available (SIGTIERRAS, 2015) and the speleological information of the Napo province (Sánchez Cortez, 2017) were used to determine this parameter. Here, areas around 500 m from the caves and karst morphologies were identified as E_1 and the rest of the study area as E_2.

Protective cover is defined by soil cover, deposits, lithologic or non-karstic geological formations over the aquifer (Doummar et al., 2012; Nekkoub et al., 2020). It is one of the natural protection parameters generally accounted for in vulnerability mapping (Doerfliger and Zwahlen, 1998). To estimate this parameter, soil and a geopedological shapefile with detailed information were considered. In particular, the geopedological shapefile contains categories associated with soil depth that allow one to establish the weight for this parameter.

Infiltration conditions are complex to estimate (Gogu and Dassargues, 2000b) because they determines how aquifer recharge occurs (Doerfliger and Zwahlen, 1998). Infiltration conditions can be estimated using the slope percentage and a land cover shapefile. A correlation between these variables allows assigning the rating values according to the original methodology for EPIK.

Karst network refers to the degree of karstification or the dissolution process of soluble rocks (limestone, dolomites, gypsum) by physiochemical interaction with water (Barea et al., 2002; Doummar et al., 2012). This parameter can be determined through direct geomorphological identification, tracer tests, or variability in water quality (Nekkoub et al., 2020). Nevertheless, no field trips could be carried out to identify and register the karst network. For that reason, geomorphological (SIGTIERRAS, 2015), speleological (Sánchez Cortez, 2017), and other related data were employed to assign a value to this parameter. Areas with geomorphological characteristics of a karst environment and the presence of caves were assigned as K_1 under the assumption that the karst network beneath the caves was well developed. And, on the other hand, the rest of the study area was assigned as K_2.

3.3. Categorization Scale

Table 6 shows the categorization scale derived from each methodology. The fact that each methodology is different makes it difficult to compare the areas corresponding to each level of vulnerability. So, for comparative purposes, a new scale was established for all vulnerability indices.

Table 6
Vulnerability classes according to Aller et al. (1987) and Doerfliger and Zwahlen (1998).

Vulnerability Class	Color	Rango DRASTIC / DRASTIC-LUC	Rango EPIK
Low		65 - 105	> 25 con $P_4 + I_{3,4}$
Moderate		105 - 146	> 25
High		146 - 187	20 - 25
Very High		187 - 230	9 - 19

Each class of vulnerability index is assigned a specific color. The scale of colors allows the user to graphically identify areas with high values and regions with low vulnerability values. This scale ranges from 0 to 1 and was obtained using the equation:

$$X_i = (X - min)/(max - min) \tag{6}$$

Where, X_i is the value derived from the new scale, X is the original value obtained from each vulnerability index, min and max are the minimum and maximum value of the vulnerability index, respectively. And, to visually identify vulnerability, 5 ranges of vulnerability class were established and each was assigned a specific color, Table 7.

Table 7
Class and color assigned for each index adapted from the new scale.

Vulnerability Class	Color	Range
Very Low		0.0 - 0.2
Low		0.2 - 0.4
Moderate		0.4 - 0.6
High		0.6 - 0.8
Very High		0.8 - 1.0

3.4. Sensitivity Analysis

Sensitivity analysis considers the contribution of individual factors and entry parameters to the outcome of an analytical model (Napolitano and Fabbri, 1996). It means that estimating the change in the output map with each change in the input helps to understand the effect of the parameters on the output of the model (Thapa et al., 2018). The two types of sensitivity analyses (Single Parameter Sensitivity and Map Removal Sensitivity) were used for this study. These methods have been used to analyze the reliability of vulnerability criteria and validate developed vulnerability maps (Tomer et al., 2019).

3.4.1. Single Parameter Sensitivity

A single parameter, or weighting factor, was developed by Napolitano and Fabbri (1996). The objective of this analysis is to determine the impact of each parameter within the vulnerability index. The effective weight of each parameter is calculated by using the following equation:

$$W_{xi} = (P_{ri} \cdot P_{wi})/V_i \cdot 100\% \tag{7}$$

Where, P_{ri} is the rating of each parameter, P_{wi} is the weight corresponding to each parameter and V_i as the vulnerability index. The Mean Percent Error shows the increase or decrease of the effective weight compared with the theoretical value. It is calculated with the following equation:

$$\text{Mean Percent Error} = (|\text{Theoretical} - \text{Real}|)/\text{Theoretical} \cdot 100\% \tag{8}$$

3.4.2. Map Removal Sensitivity

Map removal sensitivity by Lodwick et al. (1990) describes the sensitivity of the vulnerability index when removing one or more parameters from the suitability analysis. It is computed with the equation:

$$S = (|V_i/N - V_{xi}/n|)/V_i \cdot 100\% \tag{9}$$

Where V_i is the vulnerability index, N is the number of layers used for computing V_i, V_{xi} is the vulnerability index excluding one layer and n is the number of layers used for calculating V_{xi}.

4. Results and Discussion

4.1. Vulnerability Indices

The resulting values for the DRASTIC index were between 102 and 190, while for DRASTIC-LUC, the values were between 117 and 230. And, for the EPIK model, the values were between 13 and 22, as seen in Table 8.

Table 8
Statistics of the initial index.

Vulnerability Index	Mean	*Min	Max	SD
DRASTIC	157.21	102	190	18.27
DRASTIC-LUC	165.45	117	230	17.09
EPIK	17.6	13	22	2.06

*Min = Minimun, Max = Maximun, SD = Standard Deviation

Table 9 and Fig. 3 show the vulnerability maps adjusted to the new scale and the area percentage for each vulnerability class, respectively. Here, it is possible to observe areas under the same vulnerability class. The DRASTIC model shows that about 45.76% (959.40 km²) of the study area has

14

a high vulnerability, followed by 22.51% (471.96 km^2) with low exposure, and a small percent pertains to very high vulnerability (1.06%). In contrast, the DRASTIC-LUC results show that 57.47% (1204.72 km^2) has a moderate vulnerability meanwhile 23.10% (484.23 km^2) of the area was classified as low vulnerable, and 0.81% as very highly vulnerable. Compared to the other indices, the EPIK model showed a similar distribution for low to high vulnerability, so that 35.38% (741.78 km^2) has high vulnerability followed by 25.72% (539.29 km^2) as low vulnerable, and 24.24% (508.14 km^2) as moderate vulnerable. As in the previous models, the percentage of very high vulnerability is low (5.60%). This pattern was similar for the very low vulnerability with low values.

Table 9

Area distribution, in percentage and km^2, for each initial index.

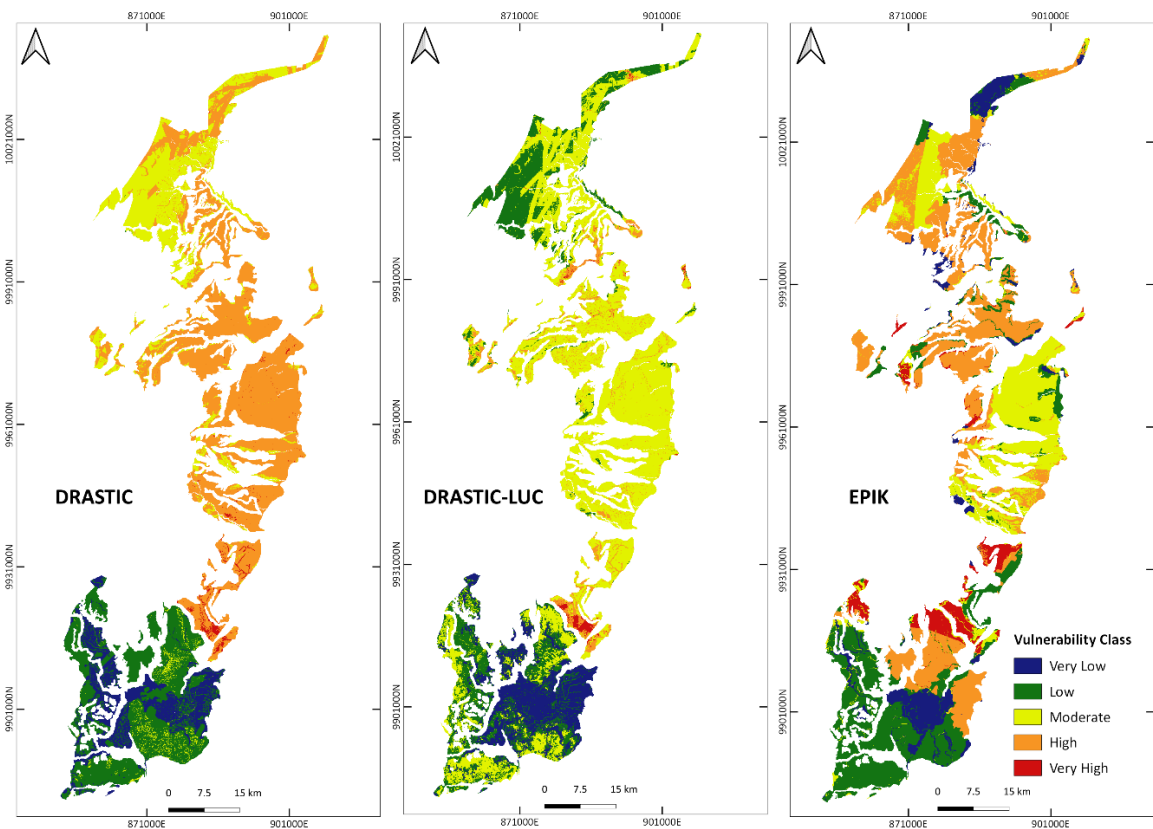| Vulnerability Class	DRASTIC (%)	DRASTIC (km^2)	DRASTIC-LUC (%)	DRASTIC-LUC (km^2)	EPIK (%)	EPIK (km^2)
Very Low	10.67	223.75	13.21	276.90	9.05	189.72
Low	22.51	471.92	23.10	484.23	25.72	539.29
Moderate	19.99	419.07	57.47	1204.72	24.24	508.14
High	45.76	959.40	5.42	113.66	35.38	741.78
Very High	1.06	22.25	0.81	16.89	5.60	117.47

Fig. 3. Vulnerability maps developed for each methodology.

4.2. Sensitivity Analysis

Table 10 summarizes the statistic values of all parameters employed for each vulnerability index. When each mean value is analyzed, the depth to the water table (9.02) appears to be the most critical contributor to the vulnerability index for DRASTIC/DRASTIC-LUC and infiltration conditions (2.86) for EPIK. Topography (2.87) and karst network (1.25), on the other hand, contribute the least to vulnerability indices. Thus, the contribution of each parameter is directly related to its weight in the final vulnerability calculation.

Table 10
Statistical summary of each model parameters.

Parameters	Symbol	Mean	Min	Max	SD
Depth to Water Table	D	9.02	9	10	0.14
Net Recharge	R	5.76	1	8	1.32
Aquifer Media	A	6.00	6	6	0.00
Soil Media	S	5.58	1	10	2.12
Topography	T	2.87	1	10	2.51
Impact of the Vadose Zone	I	4.98	3	6	1.42
Hydraulic Conductivity	C	6.93	1	10	4.27
Land and Use Cover	LUC	3.98	3	9	1.99
Epikarst	E	1.37	1	2	0.48
Protective Cover	P	2.43	2	3	0.50
Infiltration Conditions	I	2.86	2	3	0.35
Karst Network	K	1.25	1	2	0.43

4.2.1. Single Parameter Sensitivity

The change in the weighting values can be expressed both in percentage and in numerical values, and the effective weights should not be appraised on their own (Tomer et al., 2019). Statistics for effective weighting are shown in Table 11.

Table 11
Statistics of single parameter sensitivity analysis for each vulnerability index.

Parameter	Theoretical Weight	Theoretical Weight (%)	Effective Weight (%)				Real Weight	Mean Error %
			Mean	Min	Max	SD		
*D	5	21.74	31.52	24.32	44.25	4.29	7.25	44.99
R	4	17.39	16.13	2.70	27.59	4.38	3.71	7.25
A	3	13.04	12.58	9.47	17.65	1.70	2.89	3.53
S	2	8.70	7.72	1.23	16.81	3.09	1.77	11.26
T	1	4.35	2.02	0.55	8.55	1.85	0.46	53.56

I	5	21.74	16.71	10.14	22.39	3.38	3.84	23.14
C	3	13.04	13.31	2.03	22.39	7.96	3.06	2.07
D	5	17.86	27.57	20.27	39.06	3.10	7.72	54.37
R	4	14.29	14.07	2.27	24.43	3.53	3.94	1.54
A	3	10.71	11.01	7.826	15.38	1.23	3.08	2.75
S	2	7.14	6.74	1.00	14.93	2.60	1.89	5.60
T	1	3.57	1.74	0.45	7.58	1.55	0.49	51.26
I	5	17.86	14.82	7.77	20.13	3.55	4.15	17.02
C	3	10.71	12.00	1.55	20.13	7.31	3.36	12.02
LUC	5	17.86	12.06	7.32	29.41	5.83	3.38	32.47
E	3	33.33	22.10	15.79	37.50	6.64	1.99	33.69
P	1	11.11	14.26	9.52	21.43	2.95	1.28	28.35
I	3	33.33	47.22	31.58	56.25	6.15	4.25	41.67
K	2	22.22	16.43	10.00	26.67	5.16	1.48	26.06

*D = Depth to Water Table, R = Net Recharge, A = Aquifer Media, S = Soil Media, T = Topography, I = Impact of the Vadose Zone, C = Hydraulic Conductivity, LUC = Land Use and Cover, E = Epikarst, P = Protective Cover, I = Infiltration Conditions, and K = Karst Network.

These results indicate that DRASTIC parameter D dominates the vulnerability index. And, after calculating the effective weight, it is possible to notice that D became the most influential, with an effective weight of 31.52% (7.25). So that could happen because the weight and the values assigned to parameter D for the study area correspond to the water table close to the surface. This could be related to parameter I, because if the water table is close to the surface, it means that the vadose zone is smaller in size. Thus, any pollutant load would be more easily introduced into the groundwater, generating major contamination problems.

However, Table 11 shows that parameter I decreases from 5 (21.74%) to 3.84 (16.71%), with a lower error percentage. This may be due to the information used for the categorization of each parameter. This is different from the study by Kumar and Krishna (2020), which concludes that factors such as depth to the water table and vadose zone thickness are important in determining the vulnerability index. Their results show that after the effective weighting factor, these parameters contribute more to vulnerability than the other parameters. In contrast, the weight for the parameters R, A, and S reduces their theoretical weight by a small fraction. In the case of T, on the other hand, the weight drastically reduces its value (1 to 0.46), causing the error percent to be high (53.56%) and indicating that the slope is not significant in the study area of the vulnerability calculation.

For DRASTIC-LUC, a comparable situation to that described above happens with the parameters D, A, and C. With the effective weight calculated, these values increased to 7.72 (27.57%), 3.08 (11.01%), and 3.36 (12.00%), respectively. In addition, parameter R shows a decline from 4 (10.71%) to 3.94 (14.07%). On the other hand, it is interesting what happens with the parameter LUC. This parameter has a weight equal to 5 (17.86%) in the index calculation, which means LUC has a detrimental impact on the vulnerability. Nevertheless, with the recalculated weight, this value decreases to 3.38 (12.06%). This could be related to the fact that, for this study, the LUC parameter does not have a great influence on the increase in vulnerability because most of the study area contains natural areas followed by agricultural areas. This contrasts with the assignment given to the LUC parameter by Kumar and Krishna (2020), where the conditions of their study area show a predominance of agricultural areas, followed by coal mining areas, and a smaller proportion of natural areas. As a result, it indicated a significant influence on the DRASTIC-LUC model.

Nevertheless, studies carried out in Napo province show that there are activities that generate pollution, such as mining, microplastics, and inefficient wastewater treatment, that are not mapped by the entities that generate geographic information. Therefore, it would be necessary to consider a more in-depth mapping of land use and cover in NKF. This could generate more realistic results for the study area.

For the EPIK model, the value of the parameter E, despite having a high theoretical value, declined from 3 to 1.99 when the effective weight factor was calculated. The parameter K experiences a similar decline from 2 to 1.8. These results indicate that the impact on the vulnerability index of parameters E and K is less than the other parameters (P and I). This could be related to the criteria and the information that were used to obtain the E and K parameters. On the other hand, the weight of P and I increased. For I, the theoretical value was 3 (33.33%), and the new value is 4.25 (47.22%), while in the case of P, the weight changed from 1 (11.11%) to 1.28 (14.26%). It is interesting that the parameter P presents a slight increase that could be related to the soil thickness above the water table that is close to the surface. On the other hand, the considerable increase in the P parameter could be associated with the fact that slope is considered when choosing the range of this parameter. The study area is in a foothill zone where the slope in the lower zone is less than 25%, facilitating the infiltration of water and possibly pollutants. This differs from the DRASTIC model, where the slope parameter is not relevant for the calculation of vulnerability and its weight is lower.

Once the effective weight had been determined, each vulnerability index was reevaluated. The actual weight obtained from the effective weight produces a variation in each vulnerability class's area. This shows somehow more realistic results in relation to the characteristics of the study area, the ranges and ratings employed. The statistics of each model were affected in the same way, as summarized in Table 12. And, the new distribution of the vulnerability classes is shown in Fig. 4.

Table 12
Statistics of the initial index and the index after weighting factor (WF).

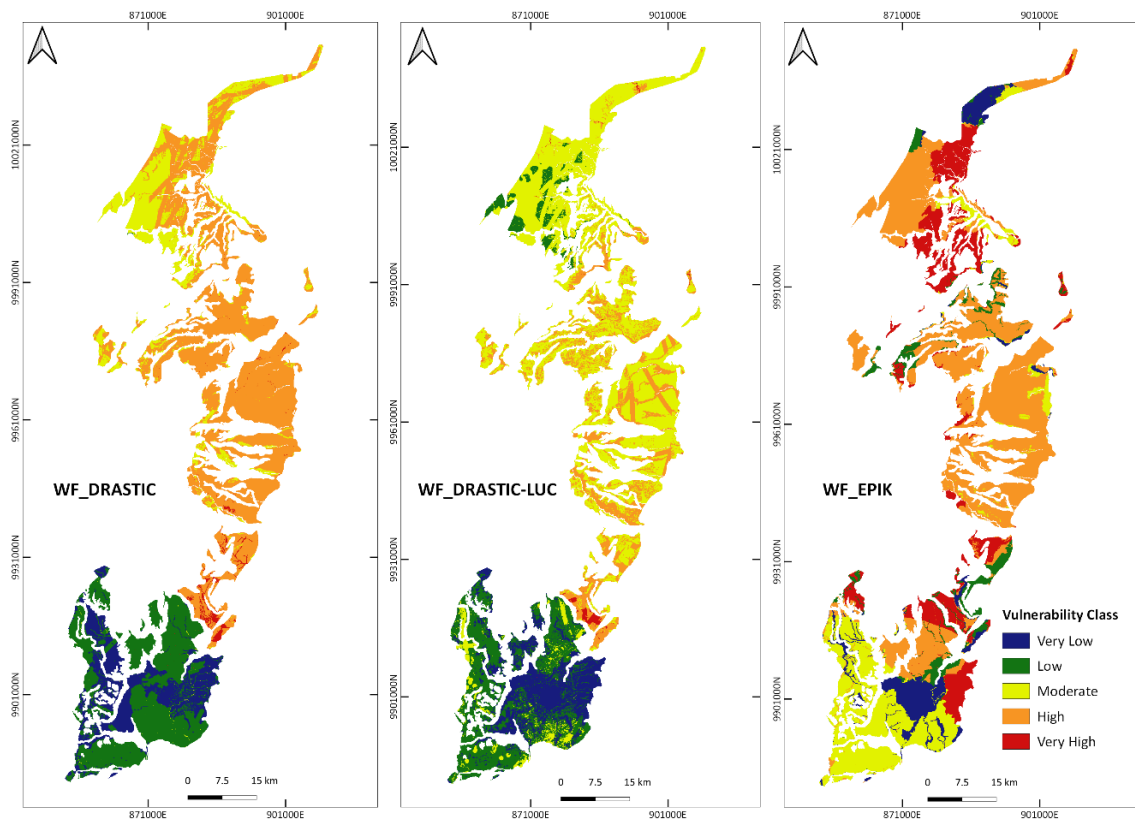| Statistics	WF_DRASTIC	WF_DRASTIC-LUC	WF_EPIK
Mean	155.26	179.77	19.82
Minimun	115.5	133.6	14.53
Maximun	195.8	236.6	23.53
SD	17.26	17.26	2.05

Fig. 4. Vulnerability maps after calculated the weighting factor.

For example, for DRASTIC, the area percentage of high vulnerability (from 45.76% to 48.95%) increased slightly compared to a moderate vulnerability (from 19.99% to 15.21%) that was reduced by the same proportion. And, the values for very low and very high vulnerability also increased to a lesser degree. It is necessary to note that the values of moderate vulnerability (from 57.47% to 48.09%) were reduced for DRASTIC-LUC, and the difference is recognizable when compared to the other classes, which reduced their values to a lesser extent. However, for high vulnerability, the value increased from 5.42% to 16.59%.

19

Whereas, for the EPIK model, the changes in the percentage distribution are more noticeable. The percentage of highly vulnerable areas increased from 35.38% to 47.98%, and similarly, the percentage of very highly vulnerable areas went from 5.60% to 17.15%. By contrast, moderate, low, and very low vulnerable areas decreased. It is especially noteworthy that low vulnerability has decreased from 25.72% to 5.91%, as can be shown in Fig. 5.
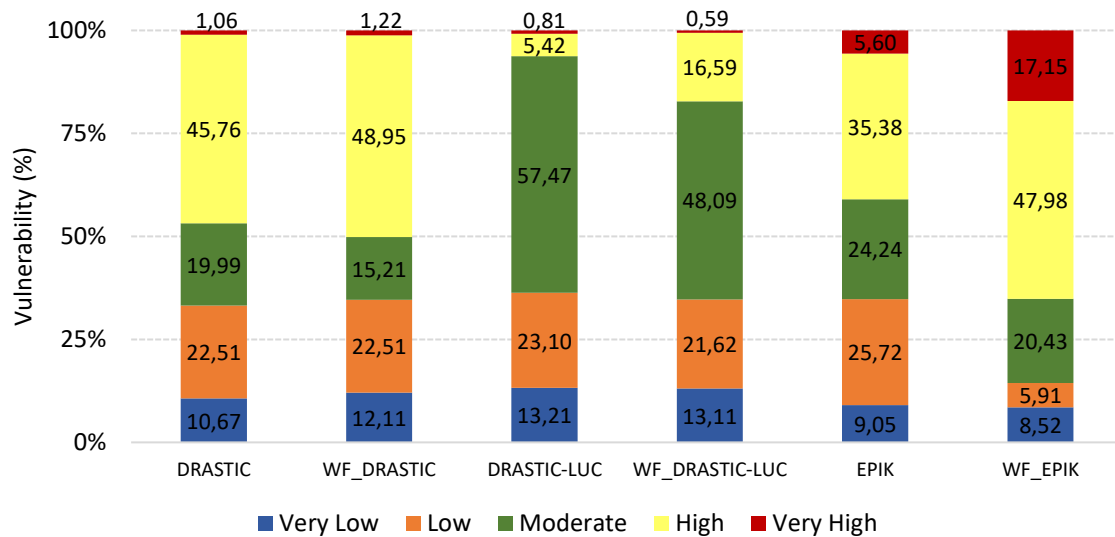

Fig. 5. Area distribution in percentage for each vulnerability index after weighting factor.

4.2.2. Map Removal Sensitivity Analysis

The first section of the analysis removed each of the parameters by applying equation (8). The findings obtained are shown in Table 13. The values corresponding to the variation index show that removing each parameter causes a degree of variation in the vulnerability index. When analyzing the DRASTIC and DRASTIC-LUC statistical data, they follow a similar pattern, D > T > C > S > LUC > I > R > A, without the LUC parameter for DRASTIC. For DRASTIC, the parameters causing the least variation are A (0.35%), R (0.61%), and I (0.64%), while for DRASTIC-LUC, they are A (0.25%), R (0.45%), I (0.56%) and LUC (0.68%). Interestingly, these parameters produce the least variation considering their weight within the index calculation (Table 2 and Table 4). On the other hand, for EPIK, the parameter that produces the least variation is E (2.13%), which contrasts with parameter I (7.97%), responsible for the greatest variation. The pattern of variation obtained from this method is I > P > K > E.

Table 13
Statistics of map removal sensitivity analysis: one parameter removed.

Parameter Removed	Variation index (%)			
	Mean	Min	Max	SD
D	2.87	1.67	4.99	0.71
T	2.04	0.96	2.29	0.31
C	1.21	0.25	2.04	0.57
S	1.10	0.00	2.18	0.51
I	0.64	0.02	1.35	0.27
R	0.61	0.00	2.20	0.50
A	0.35	0.00	0.80	0.19
D	2.15	1.11	3.79	0.44
T	1.54	0.70	1.72	0.22
C	0.97	0.08	1.56	0.40
S	0.82	0.01	1.64	0.37
LUC	0.68	0.01	2.42	0.48
I	0.56	0.01	1.09	0.22
R	0.45	0.00	1.70	0.32
A	0.25	0.00	0.67	0.11
I	7.97	2.19	10.42	1.83
P	3.69	1.19	5.16	0.96
K	3.63	0.00	5.00	1.43
E	2.13	0.64	4.17	0.68

The variation pattern for each methodology allows performing the same analysis for parameter exclusion. However, not only one parameter is removed in this case, but in sequence until only the parameter that causes the most significant degree of variation remains. The results obtained are presented in Table 14. Here is calculated a new vulnerability index with the remaining parameters, using equation (8), to estimate the variation index.

Table 14
Statistics of map removal sensitivity analysis after using a parameter.

Parameter Used							Variation index (%)			
							Mean	Min	Max	SD
DRASTIC										
D	T	C	S	I	R		0.45	0.00	0.83	0.24
D	T	C	S	I			0.36	0.00	1.37	0.33
D	T	C	S				1.87	0.00	4.79	1.56
D	T	C					3.57	0.06	9.59	2.63
D	T						1.86	0.00	8.10	1.87
D							14.84	9.52	27.73	3.78
DRASTIC-LUC										
D	T	C	S	LUC	I	R	0.25	0.00	0.67	0.11
D	T	C	S	LUC	I		0.53	0.00	2.19	0.45
D	T	C	S	LUC			0.66	0.00	2.42	0.39
D	T	C	S				0.89	0.00	4.33	0.87

D	T	C	1.88	0.00	5.37	0.98
D	T		2.20	0.00	9.40	1.78
D			15.07	7.77	26.56	3.10
EPIK						
I	P	K	2.13	0.64	4.17	0.68
I	P		6.48	0.00	10.29	3.03
I			23.91	6.58	31.25	5.48

The methods may agree on the same level of vulnerability in some areas while disagreeing in others. The notable difference may be related to the number of parameters considered by each methodology. For example, DRASTIC is based on seven hydrogeological parameters that are combined to assess vulnerability. DRASTIC-LUC includes the parameters mentioned above, plus land use and cover related to anthropogenic activities. In contrast, EPIK only consists of four parameters oriented to specific characteristics of karst environments that require a higher level of information and specificity. According to Hammouri and El-Naqa (2008), the capacity of EPIK to characterize epikarstic features is an essential distinction between it and DRASTIC when the area to be evaluated presents epikarstic traits.

The sensitivity analysis has been used to analyze the reliability of vulnerability criteria (Tomer et al., 2019). Applying these vulnerability indices may be subjective as the result depends on the author's weighting assigned to each parameter. Therefore, sensitivity analysis provided useful information on the effects of weight and rating values applied to each parameter and allowed determining the importance of the subjective aspects (Gogu and Dassargues, 2000b). The findings of Kumar and Krishna (2020), which used DRASTIC and DRASTIC-LUC, show a different pattern on the parameters causing the least variation (I > D > C > LUC > S > T > R > A). In their study, the factor that exhibited the most variation was the impact on the vadose zone, which had a weight of 5. In other words, the variations are directly associated with values assigned to each parameter and their weight in the calculation. There is no direct association between the number of removed parameters and the variation on the vulnerability index. Nonetheless, it is unfeasible to evaluate vulnerability using one or three parameters because inconsistent values can be obtained and do not reflect the reality of the study area.

When contrasted to DRASTIC or DRASTIC-LUC, EPIK employs just four parameters with a limited range of values and weights. Therefore, removing one or more parameters creates a significant variation in the final output. For example, eliminating parameter I causes more variation than removing parameter E. Nevertheless, the infiltration conditions are intriguing because they have a low vulnerability index weight but produce the highest variation when removed. That could be

related to how the protective factor operates, where low values represent high vulnerability and high values represent low vulnerability (Doerfliger et al., 1999; Doerfliger and Zwahlen, 1998).

5. Conclusions and Recommendations

In conclusion, the sensitivity analysis shows that the weight assigned to each parameter affects the final vulnerability index when the real weight is calculated. The previous values can be higher or lower than the originals. So that could be because the rating assigned can be subjective and the weight assigned does not reflect the characteristics of the study area, indicating that the weights need to be adjusted. Therefore, it is necessary to use detailed information that allows for a broader view of the study area in order to reduce subjectivity in the assignment of ranges and weights. Likewise, considering that it is necessary to have detailed data that was measured and confirmed in the field and that this study used data without validation that could have had an error, it would not be correct to say that this method is the best adapted to assess vulnerability for the study area. The information used for the DRASTIC-LUC model, on the other hand, has been measured with better accuracy and has been validated by government entities in charge of geographic information development. Therefore, after analyzing the whole process carried out to develop the vulnerability maps and the results obtained, DRASTIC-LUC is recommended as the most suitable index for the NKF. Since land use and cover have a great impact on groundwater quality, it is necessary to consider this in the vulnerability calculation.

Moreover, it is crucial to consider that around 88.35% of the area in the NKF is protected. Despite this consideration, these areas are used for agricultural, mining, and population areas that are not mapped. It is for that reason that, in further research, it would be necessary to focus on land use and cover to adapt these results to the vulnerability map. Moreover, evidence shows degradation because of these activities, and there is no research on the status of groundwater. So, considering the interaction between surface and groundwater, this resource may be in danger if the appropriate actions are not taken. The results could be used as technical studies for decision-makers when constructing infrastructures such as sanitary landfills to avoid the pollution of the surface and groundwater. On the other hand, this study paves the way for research focused on the properties of the aquifer (hydrogeological, geophysical) in the study area and complementary investigations such as groundwater quality and other relevant information (well data: pH, conductivity, nitrates, nitrites, etc.), allowing the validation of these methodologies.

6. References

Abiy, A.Z., Melesse, A.M., Behabtu, Y.M., Abebe, B., 2016. Groundwater vulnerability analysis of the tana sub-basin: An application of drastic index method, in: Melesse, A. M, Abtew, W. (Eds.), Landscape Dynamics, Soils and Hydrological Processes in Varied Climates, Springer Geography. pp. 435–461. https://doi.org/10.1007/978-3-319-18787-7_21

Al-Zabet, T., 2002. Evaluation of aquifer vulnerability to contamination potential using the DRASTIC method. Environ. Geol. 43, 203–208. https://doi.org/10.1007/s00254-002-0645-5

Alam, F., Umar, R., Ahmed, S., Dar, F.A., 2014. A new model (DRASTIC-LU) for evaluating groundwater vulnerability in parts of central Ganga Plain, India. Arab. J. Geosci. 7, 927–937. https://doi.org/10.1007/s12517-012-0796-y

Alili, L., Boukdir, A., Maslouhi, M.R., Ikhmerdi, H., 2018. Karst groundwater vulnerability mapping to the pollution: Case of Dir springs located between EL KSIBA and Ouaoumana (High Atlas, Morocco). E3S Web Conf. 37, 1–11. https://doi.org/10.1051/e3sconf/20183701004

Aller, L., Bennett, T., Lehr, J.H., Petty, R.J., Hackett, G., 1987. DRASTIC : A Standardized Method for Evaluating Ground Water Pollution Potential Using Hydrogeologic Settings.

Andreo, B., Carrasco, F., Durán, J., LaMoreaux, J., 2010. Advances in Research in Karts Media, Environmental Earth Sciences.

Andreo, B., Vías, J., Durán, J., Jiménez, P., López-Geta, J., Carrasco, F., 2008. Methodology for groundwater recharge assessment in carbonate aquifers: Application to pilot sites in southern Spain. Hydrogeol. J. 16, 911–925. https://doi.org/10.1007/s10040-008-0274-5

Andreo, B., Vías, J., López-Geta, J., Carrasco, F., Durán, J., Jiménez, P., 2004. Propuesta metodológica para la estimación de la recarga en acuíferos carbonáticos. Bol. Geol. y Min. 115, 177–186.

Awawdeh, M., Obeidat, M., Zaiter, G., 2015. Groundwater vulnerability assessment in the vicinity of Ramtha wastewater treatment plant, North Jordan. Appl. Water Sci. 5, 321–334. https://doi.org/10.1007/s13201-014-0194-6

Ayed, B., Jmal, I., Sahal, S., Brahim, F. Ben, Boughariou, E., Mokadem, N., Bouri, S., 2017. Comparison between an intrinsic and a specific vulnerability method using a GIS tool: Case of the Smar aquifer in Maritime Djeffara (southeastern Tunisia). J. Water Supply Res. Technol. - AQUA 66, 186–198. https://doi.org/10.2166/aqua.2017.081

Bakalowicz, M., 2019. Epikarst, in: Encyclopedia of Caves. Academic Press, pp. 394–398. https://doi.org/10.1016/B978-0-12-814124-3.00045-5

Baloch, M.A., Sahar, L., 2014. Development of a watershed-based geospatial groundwater specific vulnerability assessment tool. Groundwater 52, 137–147. https://doi.org/10.1111/gwat.12212

Barea, J., López-Martínez, J., Durán, J.J., 2002. Desarrollo del karst versus litoestratigrafía en los bordes norte y sur del Sistema Central español. Bol. Geol. y Min. 113, 155–164.

Barzegar, R., Asghari Moghaddam, A., Norallahi, S., Inam, A., Adamowski, J., Alizadeh, M.R., Bou Nassar, J., 2020. Modification of the DRASTIC Framework for Mapping Groundwater Vulnerability Zones. Groundwater 58, 441–452. https://doi.org/10.1111/gwat.12919

Bhuvaneswaran, C., Ganesh, A., 2019. Spatial assessment of groundwater vulnerability using DRASTIC model with GIS in Uppar odai sub-watershed, Nandiyar, Cauvery Basin, Tamil Nadu. Groundw. Sustain. Dev. 9, 100270. https://doi.org/10.1016/j.gsd.2019.100270

Boufekane, A., Saighi, O., 2018. Application of Groundwater Vulnerability Overlay and Index Methods to the Jijel Plain Area (Algeria). Groundwater 56, 143–156. https://doi.org/10.1111/gwat.12582

Buckalew, J., James, M., Lisa, S., Reed, P., 1998. Water Resources Assessment of Ecuador. Mobile District and Topographic Engineering Center, Ecuador.

Burbano, N., Becerra, S., Pasquel, E., Pérez, L., 2015. Introducción a la Hidrogeología del Ecuador. Quito, Ecuador.

Capparelli, M. V., Cabrera, M., Rico, A., Lucas-Solis, O., Alvear-S, D., Vasco, S., Galarza, E., Shiguango, Lady, Pinos-Velez, V., Pérez-González, A., Espinosa, R., Moulatlet, G.M., 2021. An Integrative Approach to Assess the Environmental Impacts of Gold Mining Contamination in the Amazon. Toxics 9, 149. https://doi.org/10.3390/toxics9070149

Capparelli, M. V., Moulatlet, G.M., de Souza Abessa, D.M., Lucas-Solis, O., Rosero, B., Galarza, E., Tuba, D., Carpintero, N., Ochoa-Herrera, V., Cipriani-Avila, I., 2019. An integrative approach to identify the impacts of multiple metal contamination sources on the Eastern Andean foothills of the Ecuadorian Amazonia. Sci. Total Environ. 709. https://doi.org/10.1016/j.scitotenv.2019.136088

Chamba, B., 2020. The First Electrical Resistivity Tomography Study Applied to an Ecuadorian Cave (Uctu Iji Changa, Tena): Insights into Amazonian Karst Systems. Universidad de Investigación Experimental de Tecnología Experimental Yachay.

Coello, X., Galárraga, R., 2002. Análisis comparativo de la vulnerabilidad del acuífero norte de Quito. XII Congr. Bras. Águas Subterrâneas 35.

Constantin, S., Toulkeridis, T., Moldovan, O.T., Villacís, M., Addison, A., 2018. Caves and karst of Ecuador–state-of-the-art and research perspectives. Phys. Geogr. 40, 28–51. https://doi.org/10.1080/02723646.2018.1461496

Davis, A.D., Long, A.J., Wireman, M., 2002. KARSTIC: A sensitivity method for carbonate aquifers in karst terrain. Environ. Geol. 42, 65–72. https://doi.org/10.1007/s00254-002-0531-1

de Castro, T., Menegasse, L., 2017. Assessment of intrinsic vulnerability to the contamination of karst aquifer using the COP method in the Carste Lagoa Santa Environmental Protection Unit, Brazil. Environ. Earth Sci. 76, 1–13. https://doi.org/10.1007/s12665-017-6760-0

Doerfliger, N., Jeannin, P.Y., Zwahlen, F., 1999. Water vulnerability assessment in karst environments: a new method of defining protection areas using a multi-attribute approach and GIS tools (EPIK method). Environ. Geol. 39, 165–176. https://doi.org/10.1007/s002540050446

Doerfliger, N., Zwahlen, F., 1998. Practical Guide - Groundwater Vulnerability Mapping in Karstic Regions (EPIK). Berna, Suiza.

Doummar, J., Margane, A., Geyer, T., Sauter, M., 2012. Protection of Jeita Spring: Vulnerability Mapping Using the COP and EPIK Methods.

Duarte, Y.A., Bautista, F., Mendoza, M.E., Delgado, C., 2013. Vulnerability and risk of contamination karstic aquifers. Trop. Subtrop. Agroecosystems 16, 243–263.

Entezari, M., Karimi, H., Gholam, H., Jafari, M., 2020. Estimation of groundwater recharge level in karstic aquifers using modified APLIS

model. Arab. J. Geosci. 13. https://doi.org/10.1007/s12517-020-5173-7

Espinoza, K., Marina, M., Fortuna, J.H., Altamirano, F., 2015. Hydrogeological and Environmental Investigations in Karst Systems. Hydrogeol. Environ. Investig. Karst Syst. 83–90. https://doi.org/10.1007/978-3-642-17435-3

Espol Tech EP, 2014. ELABORACIÓN DEL MAPA HIDROGEOLÓGICO A ESCALA 1 : 250 . 000. Guayaquil.

Farfán, H., Corvea, J.L., De Bustamante, I., 2010. Sensitivity analysis of APLIS method to compute spatial variability of karst aquifers recharge at the national park of viñales (Cuba). Environ. Earth Sci. 19–24. https://doi.org/10.1007/978-3-642-12486-0_3

Fick, S.E., Hijmans, R.J., 2017. WorldClim 2: new 1-km spatial resolution climate surfaces for global land areas. Int. J. Climatol. 37, 4302–4315. https://doi.org/10.1002/joc.5086

Foster, S., Hirata, R., Gomes, D., D'Elia, M., Paris, M., 2002. Groundwater Quality Protection, Groundwater Quality Protection. https://doi.org/10.1596/0-8213-4951-1

Freeze, R.A., Cherry, J.A., 1979. Groundwater. Prentice-Hall, Inc.

Gogu, R., Dassargues, A., 2000a. Current trends and future challenges in groundwater vulnerability assessment using overlay and index methods. Environ. Geol. 39, 549–559. https://doi.org/10.1007/s002540050466

Gogu, R., Dassargues, A., 2000b. Sensitivity analysis for the EPIK method of vulnerability assessment in a small karstic aquifer, southern Belgium. Hydrogeol. J. 8, 337–345. https://doi.org/10.1007/s100400050019

Goldscheider, N., 2005. Karst groundwater vulnerability mapping: Application of a new method in the Swabian Alb, Germany. Hydrogeol. J. 13, 555–564. https://doi.org/10.1007/s10040-003-0291-3

Goldscheider, N., Chen, Z., Auler, A.S., Bakalowicz, M., Broda, S., Drew, D., Hartmann, J., Jiang, G., Moosdorf, N., Stevanovic, Z., Veni, G., 2020. Global distribution of carbonate rocks and karst water resources. Hydrogeol. J. 1661–1677.

Hadžić, E., Lazović, N., Mulaomerović-Šeta, A., 2015. The Importance of Groundwater Vulnerability Maps in the Protection of Groundwater Sources. Key Study: Sarajevsko Polje, in: Procedia Environmental Sciences. Elsevier, pp. 104–111. https://doi.org/10.1016/j.proenv.2015.04.015

Hammouri, N., El-Naqa, A., 2008. GIS based hydrogeological vulnerability mapping of groundwater resources in Jerash area - Jordan. Geofis. Int. 47, 85–87. https://doi.org/10.22201/igeof.00167169p.2008.47.2.70

Hasan, M., Islam, M.A., Aziz Hasan, M., Alam, M.J., Peas, M.H., 2019. Groundwater vulnerability assessment in Savar upazila of Dhaka district, Bangladesh — A GIS-based DRASTIC modeling. Groundw. Sustain. Dev. 9, 100220. https://doi.org/10.1016/j.gsd.2019.100220

INAMHI, 2013. Mapa de Isoyetas media anual / Serie 81-2010. Quito, Ecuador.

Jang, W.S., Engel, B., Harbor, J., Theller, L., 2017. Aquifer vulnerability assessment for sustainable groundwater management using DRASTIC. Water (Switzerland) 9. https://doi.org/10.3390/w9100792

Jarrín, A.E., Salazar, J.G., Martínez-Fresneda Mestre, M., 2017. Evaluación del riesgo a la contaminación de los acuíferos de la Reserva Biológica de Limoncocha, Amazonía Ecuatoriana. Rev. Ambient. e Água 12, 652–665. https://doi.org/10.4136/1980-993X

Jiménez-Madrid, A., Gogu, R., Martinez-Navarrete, C., Carrasco, F., 2019. Groundwater for human consumption in karst environment: Vulnerability, protection, and management. Handb. Environ. Chem. 68, 45–63. https://doi.org/10.1007/978-3-319-77368-1_2

Kalhor, K., Ghasemizadeh, R., Rajic, L., Alshawabkeh, A., 2019. Assessment of groundwater quality and remediation in karst aquifers: A review. Groundw. Sustain. Dev. 8, 104–121. https://doi.org/10.1016/j.gsd.2018.10.004

Khan, R., Jhariya, D.C., 2019. Assessment of Groundwater Pollution Vulnerability Using GIS Based Modified DRASTIC Model in Raipur City, Chhattisgarh. J. Geol. Soc. India 93, 293–304. https://doi.org/10.1007/s12594-019-1177-x

Khosravi, K., Sartaj, M., Tsai, F.T.C., Singh, V.P., Kazakis, N., Melesse, A.M., Prakash, I., Tien Bui, D., Pham, B.T., 2018. A comparison study of DRASTIC methods with various objective methods for groundwater vulnerability assessment. Sci. Total Environ. 642, 1032–1049. https://doi.org/10.1016/j.scitotenv.2018.06.130

Kumar, A., Krishna, A.P., 2020. Groundwater vulnerability and contamination risk assessment using GIS-based modified DRASTIC-LU model in hard rock aquifer system in India. Geocarto Int. 35, 1149–1178. https://doi.org/10.1080/10106049.2018.1557259

Lenhare, B.D., Sallun Filho, W., 2019. Application of EPIK and KDI methods for identification and evaluation of karst vulnerability at Intervales State Park and surrounding region (Southeastern Brazil). Carbonates and Evaporites 34, 175–187. https://doi.org/10.1007/s13146-018-0474-6

Lerner, D.N., Harris, B., 2009. The relationship between land use and groundwater resources and quality. Land use policy 26, 265–273. https://doi.org/10.1016/j.landusepol.2009.09.005

Lessmann, J., Fajardo, J., Muñoz, J., Bonaccorso, E., 2016. Large expansion of oil industry in the Ecuadorian Amazon: biodiversity vulnerability and conservation alternatives. Ecol. Evol. 6, 4997–5012. https://doi.org/10.1002/ece3.2099

Lodwick, W.A., Monson, W., Svoboda, L., 1990. Attribute error and sensitivity analysis of map operations in geographical informations systems: Suitability analysis. Int. J. Geogr. Inf. Syst. 4, 413–428. https://doi.org/10.1080/02693799008941556

Lucas-Solis, O., Moulatlet, G.M., Guamangallo, J., Yacelga, N., Villegas, L., Galarza, E., Rosero, B., Zurita, B., Sabando, L., Cabrera, M., Gimiliani, G.T., Capparelli, M. V., 2021. Preliminary Assessment of Plastic Litter and Microplastic Contamination in Freshwater Depositional Areas: The Case Study of Puerto Misahualli, Ecuadorian Amazonia. Bull. Environ. Contam. Toxicol. https://doi.org/10.1007/s00128-021-03138-2

MAGAP, 2015. Manual de Procedimientos de Geopedología. Quito, Ecuador.

Majandang, J., Sarapirome, S., 2013. Groundwater vulnerability assessment and sensitivity analysis in Nong Rua, Khon Kaen, Thailand, using a GIS-based SINTACS model. Environ. Earth Sci. 68, 2025–2039. https://doi.org/10.1007/s12665-012-1890-x

Maqsoom, A., Aslam, B., Khalil, U., Ghorbanzadeh, O., Ashraf, H., Tufail, R.F., Farooq, D., Blaschke, T., 2020. A GIS-based DRASTIC Model and an Adjusted DRASTIC Model (DRASTICA) for Groundwater Susceptibility Assessment along the China–Pakistan Economic Corridor (CPEC) Route. ISPRS Int. J. Geo-Information 9. https://doi.org/10.3390/ijgi9050332

Marín, A.I., Andreo, B., 2015. Vulnerability to Contamination of Karst Aquifers, in: Stevanović, Z. (Ed.), Karst Aquifers - Characterization and Engineering. p. 698. https://doi.org/10.1007/978-3-319-12849-8

Merchán, P., Chiogna, G., 2017. Assessment of contamination by petroleum hydrocarbons from oil exploration and production activities in Aguarico , Ecuador. Munich, Germany.

Moustafa, M., 2019. Assessing perched aquifer vulnerability using modified DRASTIC: a case study of colliery waste in north-east England (UK). Hydrogeol. J. 27, 1837–1850. https://doi.org/10.1007/s10040-019-01932-1

Napolitano, P., Fabbri, A.G., 1996. Single-parameter sensitivity analysis for aquifer vulnerability assessment using DRASTIC and SINTACS, in: HydroGIS 96: Application of Geographic Information Systems in Hydrology and Water Resources Management

(Proceedings of the Vienna Conference, April 1996). pp. 559–566.

Nekkoub, A., Baali, F., Hadji, R., Hamed, Y., 2020. The EPIK multi-attribute method for intrinsic vulnerability assessment of karstic aquifer under semi-arid climatic conditions, case of Cheria Plateau, NE Algeria. Arab. J. Geosci. 13. https://doi.org/10.1007/s12517-020-05704-0

Oke, S.A., 2020. Regional aquifer vulnerability and pollution sensitivity analysis of drastic application to dahomey basin of Nigeria. Int. J. Environ. Res. Public Health 17. https://doi.org/10.3390/ijerph17072609

Onac, B., van Beynen, P., 2020. Caves and Karst, in: Encyclopedia of Geology. Elsevier Inc., pp. 1–15. https://doi.org/10.1016/b978-0-12-409548-9.12437-6

Oroji, B., Karimi, Z.F., 2018. Application of DRASTIC model and GIS for evaluation of aquifer vulnerability: case study of Asadabad, Hamadan (western Iran). Geosci. J. 22, 843–855. https://doi.org/10.1007/s12303-017-0082-9

Ouedraogo, I., Defourny, P., Vanclooster, M., 2016. Mapping the groundwater vulnerability for pollution at the pan African scale. Sci. Total Environ. 544, 939–953. https://doi.org/10.1016/j.scitotenv.2015.11.135

Pacheco, R., Pacheco, J., Ye, M., Cabrera, A., 2018. Groundwater Quality: Analysis of Its Temporal and Spatial Variability in a Karst Aquifer. Groundwater 56, 62–72. https://doi.org/10.1111/gwat.12546

Panagopoulos, G.P., Antonakos, A.K., Lambrakis, N.J., 2006. Optimization of the DRASTIC method for groundwater vulnerability assessment via the use of simple statistical methods and GIS. Hydrogeol. J. 14, 894–911. https://doi.org/10.1007/s10040-005-0008-x

Pathak, D.R., Hiratsuka, A., Awata, I., Chen, L., 2009. Groundwater vulnerability assessment in shallow aquifer of Kathmandu Valley using GIS-based DRASTIC model. Environ. Geol. 57, 1569–1578. https://doi.org/10.1007/s00254-008-1432-8

Pereira, D.L., Galvão, P., Lucon, T., Fujaco, M.A., 2019. Adapting the EPIK method to Brazilian Hydro(geo)logical context of the São Miguel watershed to assess karstic aquifer vulnerability to contamination. J. South Am. Earth Sci. 90, 191–203. https://doi.org/10.1016/j.jsames.2018.12.011

Ramaraju, A. V, Krishna Veni, K., 2017. Groundwater vulnerability Assessment by DRASTIC method using GIS. SSRG Int. J. Geo informatics Geol. Sci. 4, 1–8.

Ravbar, N., Goldscheider, N., 2009. Comparative application of four methods of groundwater vulnerability mapping in a Slovene karst catchment. Hydrogeol. J. 17, 725–733. https://doi.org/10.1007/s10040-008-0368-0

Rebouças, A.D.C., 1999. Groundwater resources in South America. Episodes 22, 232–237. https://doi.org/10.18814/epiiugs/1999/v22i3/011

Sahoo, S., Dhar, A., Kar, A., Chakraborty, D., 2016. Index-based groundwater vulnerability mapping using quantitative parameters. Environ. Earth Sci. 75. https://doi.org/10.1007/s12665-016-5395-x

Saida, S., Tarik, H., Abdellah, A., Farid, H., Hakim, B., 2017. Assessment of groundwater vulnerability to nitrate based on the optimised DRASTIC models in the GIS environment (Case of sidi rached basin, Algeria). Geosci. 7. https://doi.org/10.3390/geosciences7020020

Saidi, S., Bouri, S., Dhia, H. Ben, 2010. Groundwater vulnerability and risk mapping of the hajeb-jelma aquifer (central tunisia) using a gis-based drastic model. Environ. Earth Sci. 59, 1579–1588. https://doi.org/10.1007/s12665-009-0143-0

Sánchez Cortez, J.L. (Ed.), 2017. Guía Espeleológica de la Provincia Napo. Gobierno Autónomo Descentralizado de la Provincia de Napo, Universidad Regional Amazónica IKIAM, Sociedad Científica Espeleológica Ecuatoriana (ECUACAVE), Geoparque Napo-Sumaco, Tena, Ecuador.

Shirazi, S.M., Imran, H.M., Akib, S., Yusop, Z., Harun, Z.B., 2013. Groundwater vulnerability assessment in the Melaka State of Malaysia using DRASTIC and GIS techniques. Environ. Earth Sci. 70, 2293–2304. https://doi.org/10.1007/s12665-013-2360-9

SIGTIERRAS, 2015. Geomorfología. Quito, Ecuador.

Stevanović, Z., 2018. Global distribution and use of water from karst aquifers. Geol. Soc. London 466, 217–236. https://doi.org/10.1144/SP466.17

Stevanović, Z., 2015. Chapter 3: Characterization of Karst Aquifer, Karst Aquifers - Characterization and Engineering. https://doi.org/10.1007/978-3-319-12850-4

Talozi, S.A., Hijazi, H., 2013. Groundwater Contamination Hazards , Vulnerability and Risk GIS Mapping for Seven Municipalities in the Jordan Valley. Amman, Jordan. https://doi.org/10.13140/RG.2.1.4623.7843

Thapa, R., Gupta, S., Guin, S., Kaur, H., 2018. Sensitivity analysis and mapping the potential groundwater vulnerability zones in Birbhum district, India: A comparative approach between vulnerability models. Water Sci. 32, 44–66. https://doi.org/10.1016/j.wsj.2018.02.003

Tomer, T., Katyal, D., Joshi, V., 2019. Sensitivity analysis of groundwater vulnerability using DRASTIC method: A case study of National Capital Territory, Delhi, India. Groundw. Sustain. Dev. 9, 100271. https://doi.org/10.1016/j.gsd.2019.100271

Umar, R., Ahmed, I., Alam, F., 2009. Mapping groundwater vulnerable zones using modified DRASTIC approach of an alluvial aquifer in parts of central Ganga plain, western Uttar Pradesh. J. Geol. Soc. India 73, 193–201. https://doi.org/10.1007/s12594-009-0075-z

Villacís, M., Vimeux, F., Taupin, J.D., 2008. Analysis of the climate controls on the isotopic composition of precipitation (δ18O) at Nuevo Rocafuerte, 74.5°W, 0.9°S, 250 m, Ecuador. Comptes Rendus Geosci. 340, 1–9. https://doi.org/10.1016/J.CRTE.2007.11.003

Vogelbacher, A., Kazakis, N., Voudouris, K., Bold, S., 2019. Groundwater vulnerability and risk assessment in a karst aquifer of Greece using EPIK method. Environ. - MDPI 6, 1–16. https://doi.org/10.3390/environments6110116

Wei, A., Bi, P., Guo, J., Lu, S., Li, D., 2021. Modified DRASTIC model for groundwater vulnerability to nitrate contamination in the Dagujia River Basin, China. Water Supply 1–13. https://doi.org/10.2166/ws.2021.018

Zagana, E., Tserolas, P., Floros, G., Katsanou, K., Andreo, B., 2011. First outcomes from groundwater recharge estimation in evaporite aquifer in Grece with the use of APLIS method. Adv. Res. Aquat. Environ. 2, 89–96. https://doi.org/10.1007/978-3-642-24076-8

Zghibi, A., Merzougui, A., Chenini, I., Ergaieg, K., Zouhri, L., Tarhouni, J., 2016. Groundwater vulnerability analysis of Tunisian coastal aquifer: An application of DRASTIC index method in GIS environment. Groundw. Sustain. Dev. 2–3, 169–181. https://doi.org/10.1016/j.gsd.2016.10.001